

## String Phenomenology at the LHC

Luis A. Anchordoqui,<sup>1</sup> Haim Goldberg,<sup>2</sup> Dieter Lüst,<sup>3,4</sup>  
Stephan Stieberger,<sup>3</sup> and Tomasz R. Taylor<sup>2,5</sup>

<sup>1</sup>*Department of Physics,  
University of Wisconsin-Milwaukee, Milwaukee, WI 53201, USA*

<sup>2</sup>*Department of Physics,  
Northeastern University, Boston, MA 02115, USA*

<sup>3</sup>*Max-Planck-Institut für Physik  
Werner-Heisenberg-Institut, 80805 München, Germany*

<sup>4</sup>*Arnold Sommerfeld Center for Theoretical Physics  
Ludwig-Maximilians-Universität München, 80333 München, Germany*

<sup>5</sup>*Department of Physics, CERN Theory Division CH-1211 Geneva 23, Switzerland*

(Dated: September 2009)

### Abstract

We consider extensions of the standard model based on open strings ending on D-branes, with gauge bosons due to strings attached to stacks of D-branes and chiral matter due to strings stretching between intersecting D-branes. Assuming that the fundamental string mass scale is in the TeV range and the theory is weakly coupled, we review possible signals of string physics at the Large Hadron Collider.

At the time of its formulation and for years thereafter, superstring theory was regarded as a unifying framework for Planck-scale quantum gravity and TeV-scale standard model (SM) physics. Important advances were fueled by the realization of the vital role played by D-branes [1] in connecting string theory to phenomenology [2]. This has permitted the formulation of string theories with compositeness setting in at TeV scales and large extra dimensions [3].

TeV-scale superstring theory provides a brane-world description of the SM, which is localized on membranes extending in  $p + 3$  spatial dimensions (here taken to be flat), the so-called D-branes. Gauge interactions emerge as excitations of open strings with endpoints attached on the D-branes, whereas gravitational interactions are described by closed strings that can propagate in all nine spatial dimensions of string theory (these comprise flat parallel dimensions extended along the  $(p + 3)$ -branes and transverse dimensions). The apparent weakness of gravity at energies below few TeVs can then be understood as a consequence of the gravitational force “leaking” into the transverse compact dimensions of spacetime.

There are two paramount phenomenological consequences for TeV scale D-brane string physics: the emergence of Regge recurrences at parton collision energies  $\sqrt{s} \sim$  string scale  $\equiv M_s$ ; and the presence of one or more additional  $U(1)$  gauge symmetries, beyond the  $U(1)_Y$  of the SM. The latter follows from the property that the gauge group for open strings terminating on a stack of  $N$  identical D-branes is  $U(N)$  rather than  $SU(N)$  for  $N > 2$ .<sup>1</sup> In this Brief Review we exploit both these properties in order to identify “new physics” signals at the Large Hadron Collider (LHC).

Only one assumption is necessary in order to set up a solid framework: the string coupling must be small in order to rely on perturbation theory in the computations of scattering amplitudes. In this case, black hole production and other strong gravity effects occur at energies above the string scale; therefore at least a few lowest Regge recurrences are available for examination, free from interference with some complex quantum gravitational phenomena. Starting from a small string coupling, the values of standard model coupling constants are determined by D-brane configurations and the properties of extra dimensions, hence that part of superstring theory requires intricate model-building; however, as argued in [5–11], some basic properties of Regge resonances like their production rates and decay widths are completely model-independent.

To develop our program in the simplest way, we will work within the construct of a minimal model in which we consider scattering processes which take place on the (color)  $U(3)$  stack of D-branes. In the bosonic sector, the open strings terminating on this stack contain, in addition to the  $SU(3)$  octet of gluons  $g_\mu^a$ , an extra  $U(1)$  boson ( $C_\mu$ , in the notation of [12]), most simply the manifestation of a gauged baryon number symmetry. The  $U(1)_Y$  boson  $Y_\mu$ , which gauges the usual electroweak hypercharge symmetry, is a linear combination of  $C_\mu$ , the  $U(1)$  boson  $B_\mu$  terminating on a separate  $U(1)$  brane, and perhaps a third additional  $U(1)$  sharing a  $U(2)$  brane which is also a terminus for the  $SU(2)_L$  electroweak gauge bosons  $W_\mu^a$  [13]. Any vector boson  $Z'_\mu$ , orthogonal to the hypercharge, must grow a mass  $M_{Z'}$  in order to avoid long range forces between baryons other than gravity and Coulomb forces. The anomalous mass growth allows the survival of global baryon number conservation, preventing fast proton decay [14]. In what follows, the first Regge excitations

---

<sup>1</sup> For  $N = 2$  the gauge group can be  $Sp(1)$  rather than  $U(2)$ . The symplectic representation of Weinberg-Salam  $SU(2)$  reduces the required number of Higgs doublets to generate all Yukawa couplings at tree level [4].

of the gluon, quarks, and the extra  $U(1)$  boson tied to the color stack will be denoted by  $g^*$ ,  $q^*$ , and  $C^*$ , respectively.

The physical processes underlying dijet production at the LHC are the collisions of two partons  $ij$ , producing two final partons  $kl$  that fragment into hadronic jets. The corresponding  $2 \rightarrow 2$  scattering amplitudes  $\mathcal{M}(ij \rightarrow kl)$ , computed at the leading order in string perturbation theory, are collected in [8]. The amplitudes involving four gluons as well as those with two gluons plus two quarks do not depend on the compactification details of the transverse space.<sup>2</sup> All string effects are encapsulated in these amplitudes in one ‘‘form factor’’ function of Mandelstam variables  $\hat{s}$ ,  $\hat{t}$ ,  $\hat{u}$  (constrained by  $\hat{s} + \hat{t} + \hat{u} = 0$ )

$$V(\hat{s}, \hat{t}, \hat{u}) = \frac{\hat{s}\hat{u}}{\hat{t}M_s^2} B(-\hat{s}/M_s^2, -\hat{u}/M_s^2) = \frac{\Gamma(1 - \hat{s}/M_s^2) \Gamma(1 - \hat{u}/M_s^2)}{\Gamma(1 + \hat{t}/M_s^2)}. \quad (1)$$

The physical content of the form factor becomes clear after using the well-known expansion in terms of  $s$ -channel resonances [17]:

$$B(-\hat{s}/M_s^2, -\hat{u}/M_s^2) = - \sum_{n=0}^{\infty} \frac{M_s^{2-2n}}{n!} \frac{1}{\hat{s} - nM_s^2} \left[ \prod_{J=1}^n (\hat{u} + M_s^2 J) \right], \quad (2)$$

which exhibits  $s$ -channel poles associated to the propagation of virtual Regge excitations with masses  $\sqrt{n}M_s$ . Thus near the  $n$ th level pole ( $\hat{s} \rightarrow nM_s^2$ ):

$$V(\hat{s}, \hat{t}, \hat{u}) \approx \frac{1}{\hat{s} - nM_s^2} \times \frac{M_s^{2-2n}}{(n-1)!} \prod_{J=0}^{n-1} (\hat{u} + M_s^2 J). \quad (3)$$

In specific amplitudes, the residues combine with the remaining kinematic factors, reflecting the spin content of particles exchanged in the  $s$ -channel, ranging from  $J = 0$  to  $J = n + 1$ .

The amplitudes for the four-fermion processes like quark-antiquark scattering are more complicated because the respective form factors describe not only the exchanges of Regge states but also of heavy Kaluza-Klein (KK) and winding states with a model-dependent spectrum determined by the geometry of extra dimensions. Fortunately, they are suppressed, for two reasons. First, the QCD  $SU(3)$  color group factors favor gluons over quarks in the initial state. Second, the parton luminosities in proton-proton collisions at the LHC, at the parton center of mass energies above 1 TeV, are significantly lower for quark-antiquark subprocesses than for gluon-gluon and gluon-quark [6]. The collisions of valence quarks occur at higher luminosity; however, there are no Regge recurrences appearing in the  $s$ -channel of quark-quark scattering [8].

In the following we isolate the contribution to the partonic cross section from the first resonant state. Note that far below the string threshold, at partonic center of mass energies  $\sqrt{\hat{s}} \ll M_s$ , the form factor  $V(\hat{s}, \hat{t}, \hat{u}) \approx 1 - \frac{\pi^2}{6} \hat{s}\hat{u}/M_s^4$  [8] and therefore the contributions of Regge excitations are strongly suppressed. The  $s$ -channel pole terms of the average square

---

<sup>2</sup> The only remnant of the compactification is the relation between the Yang-Mills coupling and the string coupling. We take this relation to reduce to field theoretical results in the case where they exist, e.g.,  $gg \rightarrow gg$ . Then, because of the require correspondence with field theory, the phenomenological results are independent of the compactification of the transverse space. However, a different phenomenology would result as a consequence of warping one or more parallel dimensions [15, 16].

amplitudes contributing to dijet production at the LHC can be obtained from the general formulae given in [8], using Eq.(3). However, for phenomenological purposes, the poles need to be softened to a Breit-Wigner form by obtaining and utilizing the correct *total* widths of the resonances [7]. After this is done, the contributions of the various channels to the spin and color averaged matrix elements are as follows [9]

$$|\mathcal{M}(gg \rightarrow gg)|^2 = \frac{19}{12} \frac{g^4}{M_s^4} \left\{ W_{g^*}^{gg \rightarrow gg} \left[ \frac{M_s^8}{(\hat{s} - M_s^2)^2 + (\Gamma_{g^*}^{J=0} M_s)^2} + \frac{\hat{t}^4 + \hat{u}^4}{(\hat{s} - M_s^2)^2 + (\Gamma_{g^*}^{J=2} M_s)^2} \right] + W_{C^*}^{gg \rightarrow gg} \left[ \frac{M_s^8}{(\hat{s} - M_s^2)^2 + (\Gamma_{C^*}^{J=0} M_s)^2} + \frac{\hat{t}^4 + \hat{u}^4}{(\hat{s} - M_s^2)^2 + (\Gamma_{C^*}^{J=2} M_s)^2} \right] \right\}, \quad (4)$$

$$|\mathcal{M}(gg \rightarrow q\bar{q})|^2 = \frac{7}{24} \frac{g^4}{M_s^4} N_f \left[ W_{g^*}^{gg \rightarrow q\bar{q}} \frac{\hat{u}\hat{t}(\hat{u}^2 + \hat{t}^2)}{(\hat{s} - M_s^2)^2 + (\Gamma_{g^*}^{J=2} M_s)^2} + W_{C^*}^{gg \rightarrow q\bar{q}} \frac{\hat{u}\hat{t}(\hat{u}^2 + \hat{t}^2)}{(\hat{s} - M_s^2)^2 + (\Gamma_{C^*}^{J=2} M_s)^2} \right] \quad (5)$$

$$|\mathcal{M}(q\bar{q} \rightarrow gg)|^2 = \frac{56}{27} \frac{g^4}{M_s^4} \left[ W_{g^*}^{q\bar{q} \rightarrow gg} \frac{\hat{u}\hat{t}(\hat{u}^2 + \hat{t}^2)}{(\hat{s} - M_s^2)^2 + (\Gamma_{g^*}^{J=2} M_s)^2} + W_{C^*}^{q\bar{q} \rightarrow gg} \frac{\hat{u}\hat{t}(\hat{u}^2 + \hat{t}^2)}{(\hat{s} - M_s^2)^2 + (\Gamma_{C^*}^{J=2} M_s)^2} \right], \quad (6)$$

$$|\mathcal{M}(qg \rightarrow qg)|^2 = -\frac{4}{9} \frac{g^4}{M_s^2} \left[ \frac{M_s^4 \hat{u}}{(\hat{s} - M_s^2)^2 + (\Gamma_{q^*}^{J=1/2} M_s)^2} + \frac{\hat{u}^3}{(\hat{s} - M_s^2)^2 + (\Gamma_{q^*}^{J=3/2} M_s)^2} \right], \quad (7)$$

where  $g$  is the QCD coupling constant ( $\alpha_{\text{QCD}} = \frac{g^2}{4\pi} \approx 0.1$ ) and  $\Gamma_{g^*}^{J=0} = 75 (M_s/\text{TeV}) \text{ GeV}$ ,  $\Gamma_{C^*}^{J=0} = 150 (M_s/\text{TeV}) \text{ GeV}$ ,  $\Gamma_{g^*}^{J=2} = 45 (M_s/\text{TeV}) \text{ GeV}$ ,  $\Gamma_{C^*}^{J=2} = 75 (M_s/\text{TeV}) \text{ GeV}$ ,  $\Gamma_{q^*}^{J=1/2} = \Gamma_{q^*}^{J=3/2} = 37 (M_s/\text{TeV}) \text{ GeV}$  are the total decay widths for intermediate states  $g^*$ ,  $C^*$ , and  $q^*$  (with angular momentum  $J$ ) [7]. The associated weights of these intermediate states are given in terms of the probabilities for the various entrance and exit channels

$$W_{g^*}^{gg \rightarrow gg} = \frac{8(\Gamma_{g^* \rightarrow gg})^2}{8(\Gamma_{g^* \rightarrow gg})^2 + (\Gamma_{C^* \rightarrow gg})^2} = 0.44, \quad (8)$$

$$W_{C^*}^{gg \rightarrow gg} = \frac{(\Gamma_{C^* \rightarrow gg})^2}{8(\Gamma_{g^* \rightarrow gg})^2 + (\Gamma_{C^* \rightarrow gg})^2} = 0.56, \quad (9)$$

$$W_{g^*}^{gg \rightarrow q\bar{q}} = W_{g^*}^{q\bar{q} \rightarrow gg} = \frac{8\Gamma_{g^* \rightarrow gg}\Gamma_{g^* \rightarrow q\bar{q}}}{8\Gamma_{g^* \rightarrow gg}\Gamma_{g^* \rightarrow q\bar{q}} + \Gamma_{C^* \rightarrow gg}\Gamma_{C^* \rightarrow q\bar{q}}} = 0.71, \quad (10)$$

$$W_{C^*}^{gg \rightarrow q\bar{q}} = W_{C^*}^{q\bar{q} \rightarrow gg} = \frac{\Gamma_{C^* \rightarrow gg}\Gamma_{C^* \rightarrow q\bar{q}}}{8\Gamma_{g^* \rightarrow gg}\Gamma_{g^* \rightarrow q\bar{q}} + \Gamma_{C^* \rightarrow gg}\Gamma_{C^* \rightarrow q\bar{q}}} = 0.29. \quad (11)$$

Superscripts  $J = 2$  are understood to be inserted on all the  $\Gamma$ 's in Eqs.(8), (9), (10), (11). Equation (4) reflects the fact that weights for  $J = 0$  and  $J = 2$  are the same [7]. In what follows we set the number of flavors  $N_f = 6$ .

Next, we obtain the dominant  $s$ -channel pole terms of the average square amplitudes contributing to  $pp \rightarrow \gamma + \text{jet}$  [5]

$$|\mathcal{M}(qg \rightarrow q\gamma)|^2 = -\frac{1}{3}Q^2 \frac{g^4}{M_s^2} \left[ \frac{M_s^4 \hat{u}}{(\hat{s} - M_s^2)^2 + (\Gamma_{g^*}^{J=\frac{1}{2}} M_s)^2} + \frac{\hat{u}^3}{(\hat{s} - M_s^2)^2 + (\Gamma_{g^*}^{J=\frac{3}{2}} M_s)^2} \right] \quad (12)$$

and

$$|\mathcal{M}(gg \rightarrow g\gamma)|^2 = \frac{5}{3}Q^2 \frac{g^4}{M_s^4} \left[ \frac{M_s^8}{(\hat{s} - M_s^2)^2 + (\Gamma_{g^*}^{J=0} M_s)^2} + \frac{\hat{t}^4 + \hat{u}^4}{(\hat{s} - M_s^2)^2 + (\Gamma_{g^*}^{J=2} M_s)^2} \right], \quad (13)$$

where  $Q = \sqrt{1/6} \kappa \cos \theta_W$  is the product of the  $U(1)$  charge of the fundamental representation ( $\sqrt{1/6}$ ) followed by successive projections onto the hypercharge ( $\kappa$ ) and then onto the photon ( $\cos \theta_W$ ). The  $C - Y$  mixing coefficient is model dependent: in the minimal  $U(3) \times Sp(1) \times U(1)$  model it is quite small, around  $\kappa \simeq 0.12$  for couplings evaluated at the  $Z$  mass, which is modestly enhanced to  $\kappa \simeq 0.14$  as a result of RG running of the couplings up to 2.5 TeV. It should be noted that in models possessing an additional  $U(1)$  which partners  $SU(2)_L$  on a  $U(2)$  brane, the various assignment of the charges can result in values of  $\kappa$  which can differ considerably from 0.12.

Before proceeding we pause to stress that at low energies

$$|\mathcal{M}(gg \rightarrow g\gamma)|^2 \approx g^4 Q^2 C(N) \frac{\pi^4}{4} (\hat{s}^4 + \hat{t}^4 + \hat{u}^4) \quad (\hat{s}, \hat{t}, \hat{u} \ll 1). \quad (14)$$

The absence of massless poles, at  $s = 0$  *etc.*, translated into the terms of effective field theory, confirms that there are no exchanges of massless particles contributing to this process.

Events with a single jet plus missing energy ( $\cancel{E}_T$ ) with balancing transverse momenta (so-called ‘‘monojets’’) are incisive probes of new physics. As in the SM, the source of this topology is  $ij \rightarrow kZ^0$  followed by  $Z^0 \rightarrow \nu\bar{\nu}$ . Both in the SM and string theory the cross section for this process is of order  $g^4$ . Virtual KK graviton emission ( $ij \rightarrow kG$ ) involves emission of closed strings, resulting in an additional suppression of order  $g^2$  compared to  $Z^0$  emission. A careful discussion of this suppression is given in [18]. However, in some scenarios compensation for this suppression can arise from the large multiplicity of graviton emission, which is somewhat dependent on the cutoff mechanism [19–21]. Ignoring the  $Z$ -mass (i.e., keeping only transverse  $Z$ 's), the quiver contribution to  $pp \rightarrow Z + \text{jet}$  is suppressed relative to the  $pp \rightarrow \gamma + \text{jet}$  by a factor of  $\tan^2 \theta_W = 0.29$ .

The first Regge recurrence would be visible in data binned according to the invariant mass  $M$  of the final state, after setting cuts on rapidities  $|y_1|, |y_2| \leq y_{\max}$  and transverse momenta  $p_T^{1,2} > 50$  GeV, where  $y_{\max} = 2.4$  for photons and  $y_{\max} = 1$  for jets. The QCD background is calculated at the partonic level making use of the CTEQ6D parton distribution functions [22]. Standard bump-hunting methods, such as obtaining cumulative cross sections,  $\sigma(M_0) = \int_{M_0}^{\infty} \frac{d\sigma}{dM} dM$ , from the data and searching for regions with significant deviations from the QCD background, may reveal an interval of  $M$  suspected of containing a bump. With the establishment of such a region, one may calculate a signal-to-noise ratio, with the signal rate estimated in the invariant mass window  $[M_s - 2\Gamma, M_s + 2\Gamma]$ . The noise is defined as the square root of the number of background events in the same dijet mass interval for the same integrated luminosity. The LHC discovery reach (at the parton level) is encapsulated

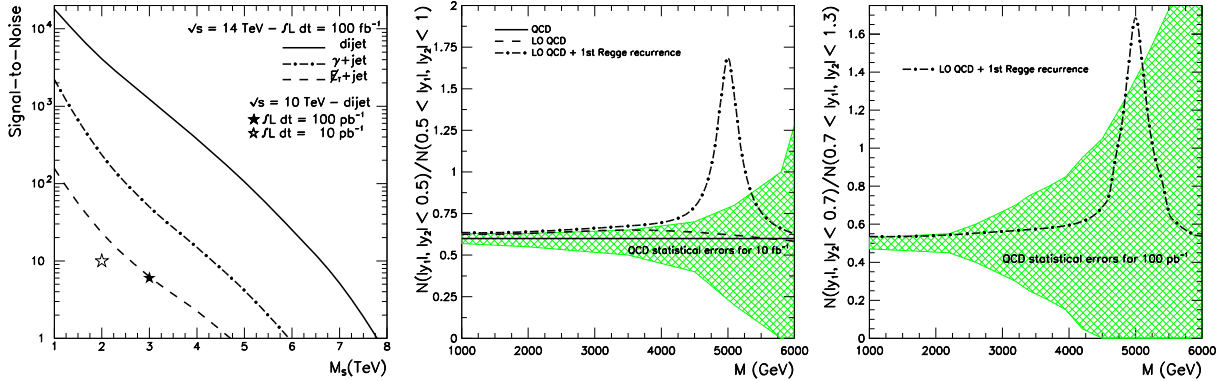


FIG. 1: *Left panel:* Signal-to-noise ratio of  $pp \rightarrow$  dijet,  $pp \rightarrow \gamma + \text{jet}$ , and  $pp \rightarrow \cancel{E}_T + \text{jet}$ , for  $\sqrt{s} = 14$  TeV,  $\sqrt{s} = 10$  TeV,  $\kappa^2 \simeq 0.02$ , and various integrated luminosities. The approximate equality of the background due to misidentified  $\pi^0$ 's and the QCD background, across a range of large  $p_T^\gamma$  as implemented in [6], is maintained as an approximate equality over a range of invariant  $\gamma$ -jet invariant masses with the rapidity cuts imposed. The monojet signal is obtained from the intermediate state  $pp \rightarrow Z^0 + \text{jet}$  multiplied by the corresponding branching ratio  $Z^0 \rightarrow \nu\bar{\nu}$ . *Middle panel:* For a luminosity of  $10 \text{ fb}^{-1}$  and  $\sqrt{s} = 14$  TeV, the expected value (solid line) and statistical error (shaded region) of the dijet ratio of QCD in the CMS detector is compared with LO QCD (dashed line) and LO QCD plus lowest massive string excitation (dot-dashed line), at a scale  $M_s = 5$  TeV. *Right panel:* The QCD statistical errors of the new dijet ratio are compared with the predictions for LO QCD plus the lowest massive string excitation (dot-dashed line) at  $\sqrt{s} = 14$  TeV, for  $100 \text{ pb}^{-1}$ .

in Fig. 1. The solid, dot-dashed, and dashed lines show the behavior of the signal-to-noise ( $S/\sqrt{B}$ ) ratio as a function of the string scale for three different event topologies (dijet,  $\gamma$ +jet, and  $\cancel{E}_T$ +jet; respectively), at  $\sqrt{s} = 14$  TeV with an integrated luminosity of  $100 \text{ fb}^{-1}$ . It is remarkable that with  $100 \text{ fb}^{-1}$  of data collection, *string scales as large as 6.8 TeV are open to discovery at the  $5\sigma$  level*. Although the discovery reach is not as high as that for dijets, the measurement of  $pp \rightarrow \gamma + \text{jet}$  and  $pp \rightarrow \cancel{E}_T + \text{jet}$  can potentially provide an interesting corroboration for the stringy origin for new physics manifest as a resonant structure in LHC data. The stars in Fig. 1 show the expected  $S/\sqrt{B}$  of dijet events for the first LHC run, at  $\sqrt{s} = 10$  TeV. For  $M_s = 3$  TeV and  $100 \text{ pb}^{-1}$  of data collected at  $\sqrt{s} = 10$  TeV, we expect  $S/\sqrt{B} = 127/20 = 6\sigma$ . For an overly conservative assumption of integrated luminosity  $\approx 10 \text{ pb}^{-1}$ , a  $S/\sqrt{B} = 204/19 > 10\sigma$  is expected for string scales as high as  $M_s = 2$  TeV. It is also remarkable that within 1 year of data collection at  $\sqrt{s} = 10$  TeV, *string scales as large as 3 TeV are open to discovery at the  $\geq 5\sigma$  level*. Once more, we stress that these results contain no unknown parameters. They depend only on the D-brane construct for the SM, and are independent of compactification details of the transverse space.

We now turn to the analysis of the angular distributions. QCD parton-parton cross sections are dominated by  $t$ -channel exchanges that produce dijet angular distributions which peak at small center of mass scattering angles. In contrast, non-standard contact interactions or excitations of resonances result in a more isotropic distribution. In terms of rapidity variables for standard transverse momentum cuts, dijets resulting from QCD processes will preferentially populate the large rapidity region, while the new processes generate events more uniformly distributed in the entire rapidity region. To analyze the details of the rapid-

ity space the DØ Collaboration [23] introduced a new parameter  $R$ , the ratio of the number of events, in a given dijet mass bin, for both rapidities  $|y_1|, |y_2| < 0.5$  and both rapidities  $0.5 < |y_1|, |y_2| < 1.0$ .<sup>3</sup> In Fig. 1 we compare the results from a full CMS detector simulation of the ratio  $R$  [25], with predictions from LO QCD and model-independent contributions to the  $q^*$ ,  $g^*$  and  $C^*$  excitations [9]. For an integrated luminosity of  $10 \text{ fb}^{-1}$  the LO QCD contributions with  $\alpha_{\text{QCD}} = 0.1$  (corresponding to running scale  $\mu \approx M_s$ ) are within statistical fluctuations of the full CMS detector simulation. (Note that the string scale is an optimal choice of the running scale which should normally minimize the role of higher loop corrections.) Since one of the purposes of utilizing NLO calculations is to fix the choice of the running coupling, we take this agreement as rationale to omit loops in QCD and in string theory. It is clear from Fig. 1 that incorporating NLO calculation of the background and the signal would not significantly change the large deviation of the string contribution from the QCD background. Very recently the CMS Collaboration optimized the dijet ratio [26]. The new ratio,  $N(|y_1|, |y_2| < 0.7)/N(0.7 < |y_1|, |y_2| < 1.3)$ , is shown in Fig. 1; string scales  $M_s < 5 \text{ TeV}$  can be probed with  $100 \text{ pb}^{-1}$  of data collection.

Although there are no  $s$ -channel resonances in  $qq \rightarrow qq$  and  $qq' \rightarrow qq'$  scattering, KK modes in the  $t$  and  $u$  channels generate calculable effective 4-fermion contact terms [8]. These in turn are manifest in an enhancement in the continuum below the string scale of the  $R$  ratio for dijet events. For  $M_{\text{KK}} \leq 3 \text{ TeV}$ , this contribution can be detected at the LHC with  $6\sigma$  significance above SM background [10]. In combination with the simultaneous observation in dijet events of a string resonance at  $M_s > M_{\text{KK}}$ , this would consolidate the stringy interpretation of these anomalies. In particular, it could serve to differentiate between a stringy origin for the resonance as opposed to an isolated structure such as a  $Z'$ , which would not modify  $R$  outside the resonant region. Moreover, because of the high multiplicity of the angular momenta (up to  $J = 2$ ), the rapidity distribution of the decay products of string excitations would differ significantly from those following decay of a  $Z'$  with  $J = 1$ . With high statistics, isolation of lowest massive Regge excitations from KK replicas (with  $J = 2$ ) may also be possible.

In terms of the perturbative cross section itself, the multiplicity of levels that one excites is limited because the scattering takes place on a particular brane from a particular helicity state. For level  $n$ , the Regge trajectory has access to  $n$  spins. For fixed  $J$  the coupling of the heavier string resonance modes  $\alpha_n^J$  decreases quadratically with energy [27], but the number of modes at each mass level  $n$  grows also quadratically. This makes  $\sum_J \alpha_n^J$  a constant independent of  $n$  and so the cross section grows linearly with energy. However, the D-brane structure with scattering confined to a single stack of D-branes may not be a valid assumption for the decay of higher mass level excited states, because there may be branching into a high multiplicity of two resonances which connect to different branes. Generally, the width of the Regge excitations will grow at least linearly with energy, whereas the spacing between levels will decrease with energy. This implies an upper limit on the domain of validity for this phenomenological approach. In particular, for a resonance  $R$  of mass  $M$ , the total width  $\Gamma_{\text{tot}} = \alpha_{\text{QCD}} \mathcal{C} M/4$ , where  $\mathcal{C} > 1$  because of the growing multiplicity of decay modes. On

---

<sup>3</sup> An illustration of the use of this parameter in a heuristic model where standard model amplitudes are modified by a Veneziano formfactor has been presented [24].

the other hand, the level spacing at mass  $M$  is  $\Delta M = M_s^2/M$ . Therefore,

$$\frac{\Gamma_{\text{tot}}}{\Delta M} = \frac{g^2}{16\pi} \mathcal{C} \left( \frac{M}{M_s} \right)^2 = \frac{g^2}{16\pi} \mathcal{C} n < 1. \quad (15)$$

For excitation of the resonance  $R$  via  $a + b \rightarrow R$ , the assumption  $\Gamma_{\text{tot}}(R) \sim \Gamma(R \rightarrow ab)$  (which underestimates the real width) yields a perturbative regime for  $n < 50$  [27]. For an increase width, the transition level can easily drop to  $n = 10$ .

Black hole intermediate states are expected to dominate  $s$ -channel scattering at trans-Planckian energies [28–31]. The number of such non-perturbative states grows faster than that of any perturbative state; e.g., the number of black hole states in 10 spacetime dimensions grows with mass like  $e^{M^{8/7}}$ , whereas the number of perturbative string states grows like  $e^M$ . Along these lines, if  $M_s \simeq 1$  TeV, semiclassical arguments seem to indicate that black hole production and evaporation would be observed at the LHC [32, 33]. However, for  $M_s \gtrsim 2$  TeV, the LHC black holes would become stringy (a.k.a. “string balls”) and their properties rather complex. String ball dynamics is framed on the context of the string  $\rightleftharpoons$  black hole correspondence principle: when the size of the black hole horizon drops below the size of the fundamental string length, an adiabatic transition occurs to an excited string state [34, 35]. Subsequently, the string will slowly lose mass by radiating massless particles with a nearly thermal spectrum at the unchanging Hagedorn temperature [36].<sup>4</sup> The continuity of the cross section at the correspondence point, at least parametrically in energy and string coupling, provides independent supportive argument for this picture [38].

*In summary*, in D-brane constructions, the full-fledged string amplitudes supplying the dominant contributions to dijet cross sections are completely independent of the details of compactification. If the string scale is in the TeV range, such extensions of the standard model can be of immediate phenomenological interest. In this Brief Review we have made use of the amplitudes evaluated near the first resonant pole to report on the discovery potential at the LHC for the first Regge excitations of the quark and gluon. Remarkably, after a few years of running, the reach of LHC in the dijet topology ( $S/N = 210/42$ ) can be as high as 6.8 TeV. This intersects with the range of string scales consistent with correct weak mixing angle found in the  $U(3) \times U(2) \times U(1)$  quiver model [13]. For string scales as high as 5.0 TeV, observations of resonant structures in  $pp \rightarrow \gamma + \text{jet}$  can provide interesting corroboration for stringy physics at the TeV-scale.

## Acknowledgments

L.A.A. is supported by the U.S. National Science Foundation Grant No PHY-0757598, and the UWM Research Growth Initiative. H.G. is supported by the U.S. National Science Foundation Grant No PHY-0757959. The research of D.L. and St.St. are supported in part by the European Commission under Project MRTN-CT-2004-005104. The research of T.R.T. is supported by the U.S. National Science Foundation Grants PHY-0600304, PHY-0757959 and by the Cluster of Excellence “Origin and Structure of the Universe” in Munich, Germany. Any opinions, findings, and conclusions or recommendations expressed in this

---

<sup>4</sup> The probability that a black hole will radiate a large string, or else that a large string would undergo fluctuation to become a black hole is very small [37].



material are those of the authors and do not necessarily reflect the views of the National Science Foundation.

---

- [1] J. Polchinski, *String Theory*, Cambridge University Press (1998).
- [2] R. Blumenhagen, B. Körs, D. Lüst and S. Stieberger, Phys. Rept. **445**, 1 (2007) [arXiv:hep-th/0610327].
- [3] I. Antoniadis, N. Arkani-Hamed, S. Dimopoulos and G.R. Dvali, Phys. Lett. B **436**, 257 (1998) [arXiv:hep-ph/9804398].
- [4] D. Cremades, L. E. Ibanez and F. Marchesano, JHEP **0307**, 038 (2003) [arXiv:hep-th/0302105].
- [5] L. A. Anchordoqui, H. Goldberg, S. Nawata and T.R. Taylor, Phys. Rev. Lett. **100**, 171603 (2008) [arXiv:0712.0386 [hep-ph]].
- [6] L. A. Anchordoqui, H. Goldberg, S. Nawata and T.R. Taylor, Phys. Rev. D **78**, 016005 (2008) [arXiv:0804.2013 [hep-ph]].
- [7] L. A. Anchordoqui, H. Goldberg and T.R. Taylor, Phys. Lett. B **668**, 373 (2008) [arXiv:0806.3420 [hep-ph]].
- [8] D. Lüst, S. Stieberger and T.R. Taylor, Nucl. Phys. B **808**, 1 (2009) [arXiv:0807.3333 [hep-th]].
- [9] L.A. Anchordoqui, H. Goldberg, D. Lüst, S. Nawata, S. Stieberger and T.R. Taylor, Phys. Rev. Lett. **101**, 241803 (2008) [arXiv:0808.0497 [hep-ph]].
- [10] L. A. Anchordoqui, H. Goldberg, D. Lust, S. Nawata, S. Stieberger and T. R. Taylor, Nucl. Phys. B **821**, 181 (2009) [arXiv:0904.3547 [hep-ph]].
- [11] D. Lust, O. Schlotterer, S. Stieberger and T. R. Taylor, arXiv:0908.0409 [hep-th].
- [12] D. Berenstein and S. Pinansky, Phys. Rev. D **75**, 095009 (2007) [arXiv:hep-th/0610104].
- [13] I. Antoniadis, E. Kiritsis and T. N. Tomaras, Phys. Lett. B **486**, 186 (2000) [arXiv:hep-ph/0004214].
- [14] D. M. Ghilencea, L. E. Ibanez, N. Irges and F. Quevedo, JHEP **0208**, 016 (2002) [arXiv:hep-ph/0205083].
- [15] B. Hassanain, J. March-Russell and J. G. Rosa, JHEP **0907**, 077 (2009) [arXiv:0904.4108 [hep-ph]].
- [16] M. Perelstein and A. Spray, arXiv:0907.3496 [hep-ph].
- [17] G. Veneziano, Nuovo Cim. A **57**, 190 (1968).
- [18] S. Cullen, M. Perelstein and M. E. Peskin, Phys. Rev. D **62**, 055012 (2000) [arXiv:hep-ph/0001166].
- [19] M. Bando, T. Kugo, T. Noguchi and K. Yoshioka, Phys. Rev. Lett. **83**, 3601 (1999) [arXiv:hep-ph/9906549].
- [20] L. A. Anchordoqui, J. L. Feng, H. Goldberg and A. D. Shapere, Phys. Rev. D **65**, 124027 (2002) [arXiv:hep-ph/0112247].
- [21] J. Hewett and T. Rizzo, JHEP **0712**, 009 (2007) [arXiv:0707.3182 [hep-ph]].
- [22] J. Pumplin, D. R. Stump, J. Huston, H. L. Lai, P. Nadolsky and W. K. Tung, JHEP **0207**, 012 (2002) [arXiv:hep-ph/0201195].
- [23] B. Abbott *et al.* [D0 Collaboration], Phys. Rev. Lett. **82**, 2457 (1999) [arXiv:hep-ex/9807014].
- [24] P. Meade and L. Randall, JHEP **0805**, 003 (2008) [arXiv:0708.3017 [hep-ph]].
- [25] S. Esen and R. Harris, CMS Note 2006/071.
- [26] A. Bhatti *et al.*, J. Phys. G **36**, 015004 (2009) [arXiv:0807.4961 [hep-ex]].

- [27] F. Cornet, J. I. Illana and M. Masip, Phys. Rev. Lett. **86**, 4235 (2001) [arXiv:hep-ph/0102065].
- [28] D. Amati, M. Ciafaloni and G. Veneziano, Phys. Lett. B **197**, 81 (1987).
- [29] G. 't Hooft, Phys. Lett. B **198**, 61 (1987).
- [30] D. Amati, M. Ciafaloni and G. Veneziano, Phys. Lett. B **289**, 87 (1992).
- [31] D. Amati, M. Ciafaloni and G. Veneziano, JHEP **0802**, 049 (2008) [arXiv:0712.1209 [hep-th]].
- [32] S. Dimopoulos and G. Landsberg, Phys. Rev. Lett. **87**, 161602 (2001) [arXiv:hep-ph/0106295].
- [33] S. B. Giddings and S. D. Thomas, Phys. Rev. D **65**, 056010 (2002) [arXiv:hep-ph/0106219].
- [34] G. T. Horowitz and J. Polchinski, Phys. Rev. D **55**, 6189 (1997) [arXiv:hep-th/9612146].
- [35] T. Damour and G. Veneziano, Nucl. Phys. B **568**, 93 (2000) [arXiv:hep-th/9907030].
- [36] D. Amati and J. G. Russo, Phys. Lett. B **454**, 207 (1999) [arXiv:hep-th/9901092].
- [37] G. T. Horowitz and J. Polchinski, Phys. Rev. D **57**, 2557 (1998) [arXiv:hep-th/9707170].
- [38] S. Dimopoulos and R. Emparan, Phys. Lett. B **526**, 393 (2002) [arXiv:hep-ph/0108060].